

Additive Schwarz Domain-Decomposition method with embedded small scales for Diffusion Equation

Jürgen Geiser and Susanne Kilian

Department of Mathematics, Humboldt Universität zu Berlin,
Unter den Linden 6, D-10099 Berlin, Germany
geiser@mathematik.hu-berlin.de kilian@mathematik.hu-berlin.de

Zusammenfassung We present a convergence and error bound study for domain-decomposition methods with very small domains. The idea is to apply very fast solver methods for strips with $h \ll \epsilon$ and to exploit optimized local smoothing properties on the interface for $h \approx \epsilon$. We apply the results in some applications for 2 dimensional domains.

Keywords. Additive Schwarz method, Schwarz waveform relaxation method, heat equation, convection-diffusion equation, a priori error estimates, crystal-growth apparatus.

AMS subject classifications. 80A20, 80M25, 74S10, 76R50, 35J60, 35J65, 65M99, 65Z05, 65N12

1 Introduction

The first known method for solving partial differential equations on overlapping domains is the Schwarz method due to [27] in 1869. The method has regained its popularity due to the development of the computational numerical algorithms especially with regard to modern parallel computer architectures. We concentrate on the Additive Schwarz domain decomposition and interpret the error analysis with the Schwarz waveform relaxation method for an h overlap. Some accurate results can be derived and numerical example complete our theoretical results.

2 Model-Problem

The motivation for the study presented below is based on a computational simulation of heat-transfer [12] and convection-diffusion-reaction-equations [10], [17], [18] and [16].

We concentrate on a stationary heat-equation, given by

$$-\nabla \cdot D \nabla u = f, \quad \text{in } \Omega, \quad (1)$$

$$u = 0, \quad \text{on } \partial\Omega. \quad (2)$$

The unknown $u = u(x, t)$ is considered in $\Omega \subset \mathbb{R}^2$ or \mathbb{R}^3 , where $\Omega = [0, L]^2$ or $\Omega = [0, L]^3$. The diffusion coefficient D is a constant factor, but anisotropic in the different spatial directions.

The aim of this paper is to present a accurate apriori errors for small overlapping domains with $\epsilon \approx h$.

Now we introduce the domain-decomposition method as basic idea for a splitting method which decomposes complex domains and solves them effectively.

3 Schwarz wave form relaxation for the solution of spatial dependent diffusion equation

In this section we present the necessary conditions for the convergence of the overlapping Schwarz wave form relaxation method for the solution of the stationary diffusion equation with bounded coefficients.

We consider the stationary one-dimensional convection-diffusion-reaction equation, given by

$$Du_{xx} - \nu u_x - \lambda u = 0, \quad (3)$$

defined on the domain Ω , where $\Omega = [0, L]$, with the following boundary conditions

$$u(0, t) = f_1, \quad u(L, t) = f_2.$$

The generalisation can also be done for multi-dimensions, see [5].

To solve the model problem using overlapping Schwarz wave form relaxation method, we subdivide the domain Ω in two overlapping sub-domains $\Omega_1 = [0, L_2]$ and $\Omega_2 = [L_1, L]$, where $L_1 < L_2$ and $\Omega_1 \cap \Omega_2 = [L_1, L_2]$ is the overlapping region for Ω_1 and Ω_2 .

To start the wave form relaxation algorithm we consider first the solution of the model problem (3) over Ω_1 and Ω_2 as follows

$$\begin{aligned} Dv_{xx} - \nu v_x - \lambda v &= 0 \text{ over } \Omega_1, \\ v(0) &= f_1, \\ v(L_2) &= w(L_2), \end{aligned} \quad (4)$$

$$\begin{aligned} Dw_{xx} - \nu w_x - \lambda w &= 0 \text{ over } \Omega_2, \\ w(L_1) &= v(L_1), \\ w(L) &= f_2, \end{aligned} \quad (5)$$

where $v(x) = u(x)|_{\Omega_1}$ and $w(x) = u(x)|_{\Omega_2}$.

Then the Schwarz wave form relaxation is given by

$$\begin{aligned} Dv_x^{k+1} - \nu v_x^{k+1} - \lambda v^{k+1} &= 0 \text{ over } \Omega_1, \\ v^{k+1}(0) &= f_1, \\ v^{k+1}(L_2) &= w^k(L_2), \end{aligned} \quad (6)$$

$$\begin{aligned} Dw_x^{k+1} - \nu w_x^{k+1} - \lambda w^{k+1} &= 0 \text{ over } \Omega_2, \\ w^{k+1}(L_1) &= v^k(L_1), \\ w^{k+1}(L) &= f_2. \end{aligned} \quad (7)$$

We are interested in estimating the decay of the error of the solution over the overlapping subdomains, later for a small overlap of h .

Let us assume that $e^{k+1}(x) = u(x) - v^{k+1}(x)$ and $d^{k+1}(x) = u(x) - w^{k+1}(x)$ are the errors of (6) and (7) over Ω_1 and Ω_2 respectively. The corresponding differential equations satisfied by $e^{k+1}(x)$ and $d^{k+1}(x)$ are

$$\begin{aligned} D e_{xx}^{k+1} - \nu e_x^{k+1} - \lambda e^{k+1} &= 0 \text{ over } \Omega_1, \\ e^{k+1}(0) &= 0, \\ e^{k+1}(L_2) &= d^k(L_2), \end{aligned} \tag{8}$$

$$\begin{aligned} D d_{xx}^{k+1} - \nu d_x^{k+1} - \lambda d^{k+1} &= 0 \text{ over } \Omega_2, \\ d^{k+1}(L_1) &= e^k(L_1), \\ d^{k+1}(L) &= 0. \end{aligned} \tag{9}$$

We define for bounded functions $h(x) : \Omega \rightarrow \mathbf{R}$ the norm

$$\|h(\cdot)\|_\infty := \sup_{x \in \Omega} |h(x)|.$$

The convergence and error-estimates of e^{k+1} and d^{k+1} given by (8) and (9) respectively, are presented in the following theorem

Theorem 1. *Let e^{k+1} and d^{k+1} be the error from the solution of the subproblems (4) and (5) by Schwarz wave form relaxation over Ω_1 and Ω_2 , respectively, then*

$$\|e^{k+2}(L_1)\|_\infty \leq \gamma \|e^k(L_1)\|_\infty,$$

and

$$\|d^{k+2}(L_2)\|_\infty \leq \gamma \|d^k(L_1)\|_\infty,$$

where

$$\gamma = \frac{\sinh(\beta L_1) \sinh(\beta(L_2 - L))}{\sinh(\beta L_2) \sinh(\beta(L_1 - L))} < 1,$$

with $\beta = \frac{\sqrt{\nu^2 + 4D\lambda}}{2D}$.

Proof. In order to estimate the errors e^{k+1} and d^{k+1} , we consider the following differential equations containing \hat{e}^{k+1} and \hat{d}^{k+1} :

$$\begin{aligned} D \hat{e}_{xx}^{k+1} - \nu \hat{e}_x^{k+1} - \lambda \hat{e}^{k+1} &= 0 \text{ over } \Omega_1, \\ \hat{e}^{k+1}(0) &= 0, \\ \hat{e}^{k+1}(L_2) &= \|d^k(L_2)\|_\infty, \end{aligned} \tag{10}$$

The same could be also done for \hat{d}^{k+1} .

The solution of $\hat{e}^{k+1}(x)$ and $\hat{d}^{k+1}(x)$ are given as

$$\hat{e}^{k+1}(x) = e^{(x-L_2)\alpha} \frac{\sinh(\beta x)}{\sinh(\beta L_2)} \|d^k(L_2)\|_\infty,$$

and

$$\hat{d}^{k+1}(x) = e^{(x-L_1)\alpha} \frac{\sinh \beta(x-L)}{\sinh \beta(L_1-L)} \|e^k(L_1)\|_\infty,$$

respectively.

Then

$$|e^{k+1}(x)| \leq e^{(x-L_2)\alpha} \frac{\sinh(\beta x)}{\sinh(\beta L_2)} \|d^k(L_2)\|_\infty, \quad (11)$$

and

$$|d^{k+1}(x)| \leq e^{(x-L_1)\alpha} \frac{\sinh \beta(x-L_1)}{\sinh \beta(L_1-L)} \|e^k(L_1)\|_\infty. \quad (12)$$

Therefore we can estimate the parts by replacing the maximum value at $x = L_2$, i.e.

$$\|e^{k+2}(L_1)\| \leq \frac{\sinh(\beta L_1)}{\sinh(\beta L_2)} \frac{\sinh \beta(L_2-L)}{\sinh \beta(L_1-L)} \|e^k(L_1)\|_\infty.$$

Similarly for $d^{k+1}(x)$ we conclude that

$$\|d^{k+2}(L_2)\| \leq \frac{\sinh(\beta L_1)}{\sinh(\beta L_2)} \frac{\sinh \beta(L_2-L)}{\sinh \beta(L_1-L)} \|d^k(L_1)\|_\infty.$$

Theorem 1 shows that the convergence of the overlapping Schwarz method depends on γ . The result can also be used for a small overlap with $L_2 - L_1 = h$, where h is the grid-length of the underlying discretisation. Such an overlap is given for the additive Schwarz method and one can use such results as a first estimate for the accuracy of the Schwarz-method, see [3].

Remark 1. The results of Theorem 1 can be generalised for bounded parameters D and v , if we can estimate the parameters as $\hat{D} = \sup_{x \in \Omega} D(x)$, $\hat{v} = \sup_{x \in \Omega} v(x)$.

4 Numerical Results

In this section we will present the numerical results for the solution of several model problems using the presented methods.

All examples are based on the two-dimensional diffusion equation given by

$$\begin{aligned} -\nabla D_i \nabla u &= 0, & \text{in } \Omega_i, \\ -\nabla D_\epsilon \nabla u &= f, & \text{in } \Omega_\epsilon, \\ u &= 0, & \text{on } \partial\Omega, \end{aligned} \quad (13)$$

for a slightly overlapping subdivision of a given domain Ω into ‘big’ subdomains Ω_i , $i = 1, \dots, N$, and a ‘small’ subdomain Ω_ϵ with diameter ϵ . The diffusion-coefficients for the single subdomains are chosen differently.

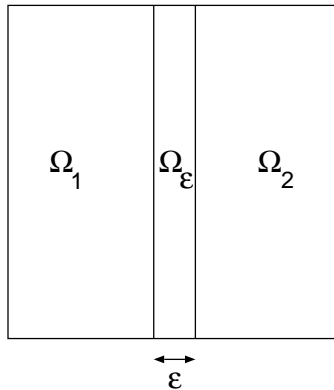


Abbildung 1. 'Geometry 1' with 3 subdomains

4.1 First example: Diffusion-equation

The unit square is decomposed into 3 single subdomains as illustrated in figure 1 with a small strip Ω_ϵ of diameter $\epsilon = 0.1$ or 0.01 in the middle. The corresponding diffusion-coefficients are set to $D_i = 1.0$ in Ω_i , $i = 1, 2$, and $D_\epsilon = 0.1, 0.01, 0.001$ in Ω_ϵ .

The right hand side is defined by $f = 1$. We restrict on pure Dirichlet boundary conditions with zero boundary.

The problem is solved by the SCARC-algorithm which is based on a data-parallel global MG-method with smoothing by optimized local MG-methods, see [19], [20] and [1]. The smoothing of the local MG-methods is achieved by GSADI-methods. Two pre- and postprocessing steps are performed in each MG-step.

For each constellation of the ϵ and D_ϵ we consider the grid refinement levels $l = 3, 4, 5, 6, 7$. The resulting convergence rates are indicated in table 1.

For the different values of ϵ we have the following grid resolutions:

- $\epsilon = 0.1$: For $\Omega_\epsilon = [0.45, 0.55] \times [0, 1]$, the finest step size h_{min} ranges from $0.125 * 10^{-1}$ for refinement level 3 up to $0.781 * 10^{-3}$ for refinement level 7. The maximum aspect ratio amounts to 10.
- $\epsilon = 0.01$: For $\Omega_\epsilon = [0.495, 0.505] \times [0, 1]$, the finest step size h_{min} ranges from $0.125 * 10^{-2}$ for refinement level 3 up to $0.781 * 10^{-4}$ for refinement level 7. The maximum aspect ratio amounts to 100.

Figure 2 illustrates the refinement of the single subdomains as well as the resulting solution for level $l = 5$ and $\epsilon = 0.1$.

To demonstrate the effect of the different diffusion-coefficients $D_\epsilon = 0.1$ and $D_\epsilon = 0.001$, a horizontal cut of the solution at $y=0.5$ is indicated in figure 3.

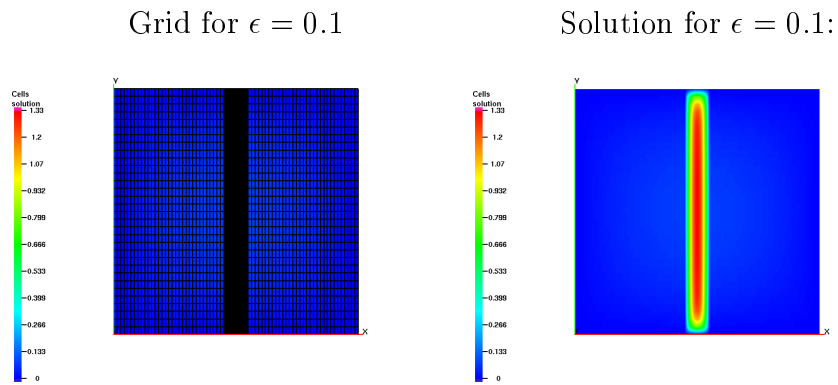


Abbildung 2. 'Geometry 1': Grid and solution for level 5 and $\epsilon = 0.1$.

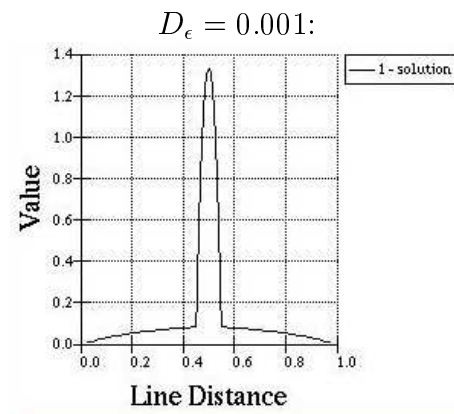


Abbildung 3. 'Geometry 1': Horizontal cut through the solution at $y = 0.5$ for level 5 with $\epsilon = 0.1$.

ϵ	MG-Level	Convergence-rate		
		$D_\epsilon = 0.1$	$D_\epsilon = 0.01$	$D_\epsilon = 0.001$
0.1	3	0.018	0.040	0.041
	4	0.025	0.015	0.019
	5	0.030	0.020	0.031
	6	0.035	0.028	0.034
	7	0.039	0.034	0.044
0.01	3	0.078	0.021	0.016
	4	0.073	0.022	0.015
	5	0.068	0.021	0.015
	6	0.063	0.019	0.016
	7	0.060	0.018	0.017

Tabelle 1. 'Geometry 1': Convergence rates of SCARC with $\epsilon = 0.1, 0.01$.

4.2 Second example: Steady state Diffusion-equation with ϵ -Domains

We consider the two-dimensional diffusion equation 13 for the subdivision of the unit square shown in figure 4. The thickness of the small strip in the middle is set to $\epsilon = 0.1$ or 0.01 .

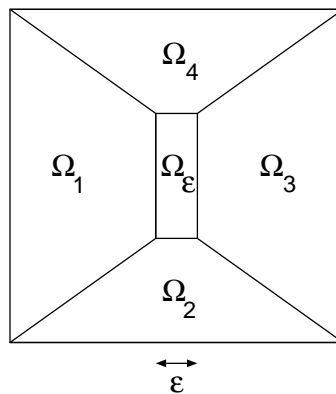


Abbildung 4. 'Geometry 2' with 5 subdomains

The diffusion-coefficients in Ω_i , $i = 1, \dots, 4$, are set to $D_i = 1.0$. For Ω_ϵ we analyze the cases $D_\epsilon = 0.1, 0.01, 0.001$. Again, we consider the grid refinement levels $l = 3, 4, 5, 6, 7$. The resulting convergence rates from SCARC are summarized in table 2.

For the different values of ϵ we have the following grid resolutions:

- $\epsilon = 0.1$: For $\Omega_\epsilon = [0.45, 0.55] \times [0.3, 0.7]$, the finest step size h_{min} ranges from $0.125 * 10^{-1}$ for refinement level 3 up to $0.781 * 10^{-3}$ for refinement level 7. The maximum aspect ratio amounts to 5.2 for level 7.
- $\epsilon = 0.01$: For $\Omega_\epsilon = [0.495, 0.505] \times [0.3, 0.7]$, the finest step size h_{min} ranges from $0.125 * 10^{-2}$ for refinement level 3 up to $0.781 * 10^{-4}$ for refinement level 7. The maximum aspect ratio amounts to 41.5 for level 7.

ϵ	MG-Level	Convergence-rate		
		$D_\epsilon = 0.1$	$D_\epsilon = 0.01$	$D_\epsilon = 0.001$
0.1	3	0.029	0.031	0.031
	4	0.038	0.042	0.074
	5	0.052	0.064	0.064
	6	0.062	0.070	0.072
	7	0.071	0.078	0.084
0.01	3	0.016	0.013	0.013
	4	0.021	0.019	0.020
	5	0.036	0.035	0.038
	6	0.062	0.061	0.069
	7	0.107	0.105	0.112

Tabelle 2. 'Geometry 2': Convergence rates of SCARC with $\epsilon = 0.1$ and $\epsilon = 0.01$.

Figures 5 and 6 illustrate the grid refinement and the solution as well as its horizontal cut along $y=0.5$ for $l = 5$ and $\epsilon = 0.1$.

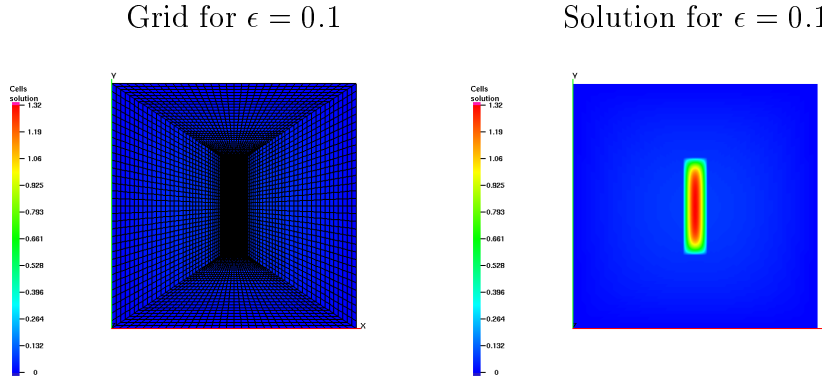


Abbildung 5. 'Geometry 2': Grid and solution for level 5, $\epsilon = 0.1$ and $D_\epsilon = 0.001$.

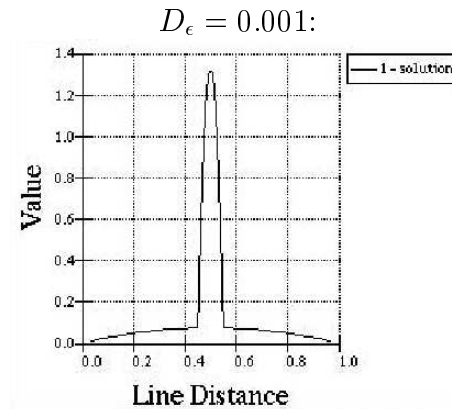


Abbildung 6. 'Geometry 2': Horizontal cut through the solution at $y = 0.5$ for level 5 and $\epsilon = 0.1$ and $D_{\epsilonpsilon} = 0.1, 0.001$.

4.3 Third example: Simpler Crystal-growth apparatus.

We consider the two-dimensional diffusion equation 13 on the more complex domain illustrated in figure 7 which modelizes a crystal-growth apparatus. This domain is subdivided into 63 subdomains. The size of the heating-strip Ω_ϵ is taken as $\epsilon = 0.3$.

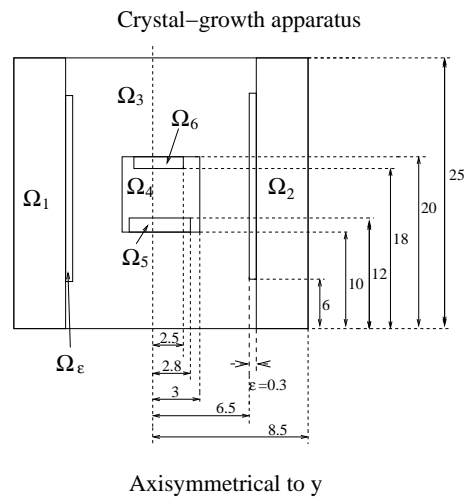


Abbildung 7. 'Geometry 3': The apparatus of the crystal-growth with small ϵ .

The heating source on the ϵ -strip is given as $f = 1$, the boundary-conditions are purely dirichlet-boundary-conditions with zero boundary.

The coefficients are $D_1 = D_2 = 0.3$ (*insulation*), $D_3 = D_\epsilon = 10.0$ (*graphit*), $D_4 = 0.001$ (*gas*), $D_5 = 50.0$ (*silicon-powder*).

Table 3 compares the convergence rates of SCARC with those of a data-parallel multigrid method with a blockwise ILU-smoothing for different diffusions coefficients $D_\epsilon = 1.0, 0.1, 0.01, 0.001$ in Ω_ϵ .

D_ϵ	MG-Level	Convergence-rate	
		Block-ILU-MG	SCARC
0.001	3	0.138	0.098
	4	0.128	0.098
	5	0.122	0.075
	6	0.125	0.075
	7	0.130	0.075
0.01	3	0.133	0.099
	4	0.128	0.097
	5	0.125	0.075
	6	0.132	0.075
	7	0.144	0.075
0.1	3	0.136	0.100
	4	0.134	0.088
	5	0.155	0.076
	6	0.174	0.076
	7	0.189	0.075
1.0	3	0.141	0.110
	4	0.152	0.085
	5	0.174	0.074
	6	0.191	0.074
	7	0.200	0.076
1.0	3	0.161	0.112
	4	0.172	0.101
	5	0.184	0.098
	6	0.191	0.116
	7	0.207	0.112

Tabelle 3. 'Geometry 3': Convergence rates of Block-ILU-MG and SCARC on the crystal-growth apparatus with $\epsilon = 0.3$.

For the different grid refinement levels the resulting finest step sizes h_{min} as well as the total number of nodes N_{total} are shown in table 4. The maximum of aspect ratio amounts to 30.

In the next figure 8 we compare the computations for different diffusion-parameters in the gas-chamber.

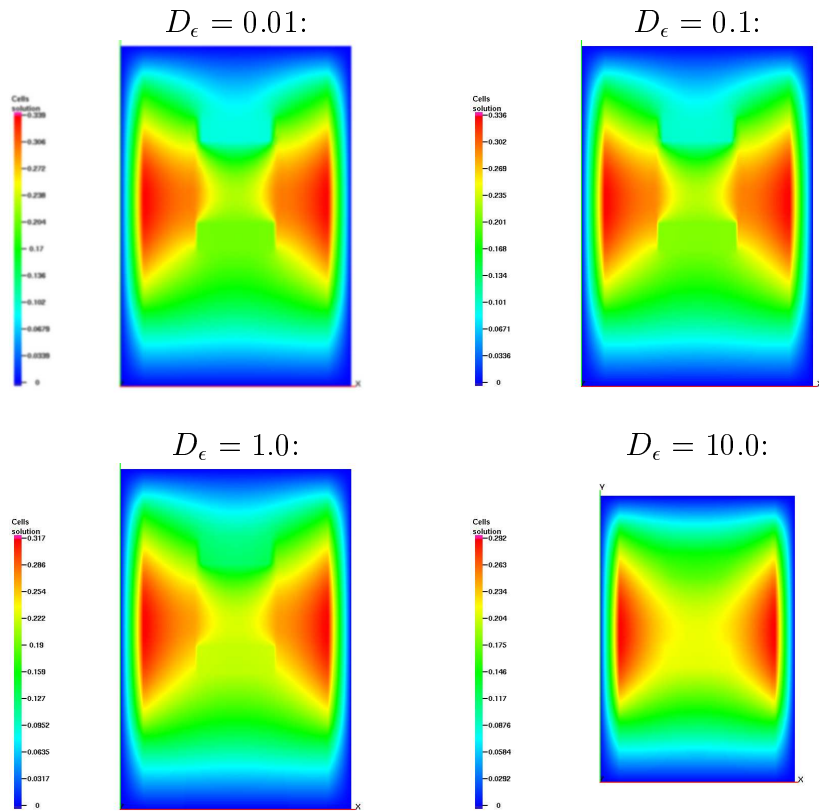


Abbildung 8. 'Geometry 3': Solution for different coefficients $D_\epsilon = 0.01, 0.1, 1.0, 10.0$.

MG-Level	h_{min}	N_{total}
3	0.245-1	4.161
4	0.125-1	16.385
5	0.625-2	65.025
6	0.315-2	259.073
7	0.156-2	1.034.241

Tabelle 4. 'Geometry 3': Grid resolutions for different multigrid levels.

In figures 8 presents different diffusion coefficients for the small heating-strip. Because of the increasing diffusion coefficient in the gas-chamber the temperature can smooths more over the area.

In the next experiment we deal with a larger heating-strip to increase the temperature in the gas-chamber.

4.4 Fourth example: Simpler Crystal-growth apparatus (larger heating-strip).

We consider the same test constellation as described in the third example, but now with a larger heating source, $\epsilon = 2.0$ instead of $\epsilon = 0.3$, see figure 9.

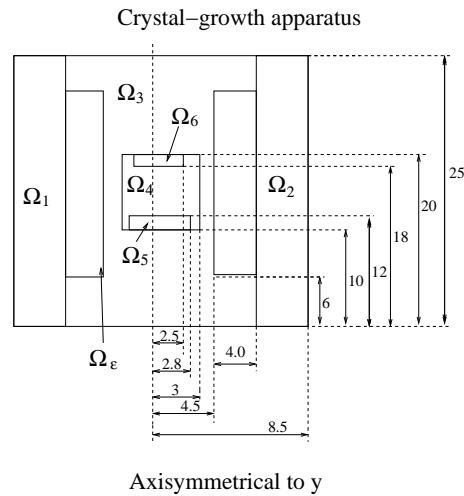


Abbildung 9. 'Geometry 4': The apparatus of the crystal-growth with big ϵ .

The convergence rates of Block-ILU-MG and SCARC are indicated in table 5.

In table 5 we obtain decreasing convergence-rates for finer grid-meshes. We can also see the results for different diffusion coefficients. So at least we have

MG-Level	Convergence-rate				
	$D_\epsilon = 0.001$	$D_\epsilon = 0.01$	$D_\epsilon = 0.1$	$D_\epsilon = 1.0$	$D_\epsilon = 10.0$
3	0.098	0.099	0.100	0.110	0.110
4	0.098	0.097	0.088	0.085	0.086
5	0.075	0.075	0.076	0.074	0.074
6	0.076	0.079	0.076	0.110	0.130
7	0.075	0.076	0.075	0.076	0.076

Table 5. 'Geometry 4': Convergence rates of SCARC on the crystal-growth apparatus with $\epsilon = 2.0$ for different diffusion coefficients.

a stable method based on a small overlap but stabilised with local multi-grid methods.

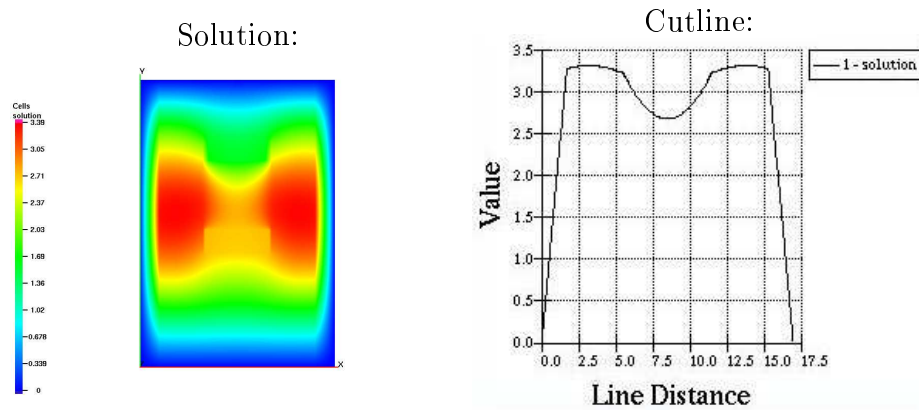


Abbildung 10. 'Geometry 4': Solution and cutline for $D_\epsilon = 10.0$

In figure 10 we see a more regular diffusion of the heat over the gas-chamber. The heating-temperature in the gas-chamber is nearly constant. So larger heating-strip can bring more stability to the adjoint regions.

In a last example we assume the heating-strip near to the gas-chamber.

4.5 Fifth example: Simpler Crystal-growth apparatus (heating strip near to the gas-chamber).

We consider the geometry in figure 11 with a heating strip near the gas-chamber with the same settings as described above. The diameter of the heating-strip is $\epsilon = 0.3$.

Table 6 lists the convergence rates of SCARC for grid refinement level 6 and different diffusion coefficients in the ϵ -strip. Figure ?? illustrates the solution and a cutline through $y = 15.0$ for $D_\epsilon = 10.0$.

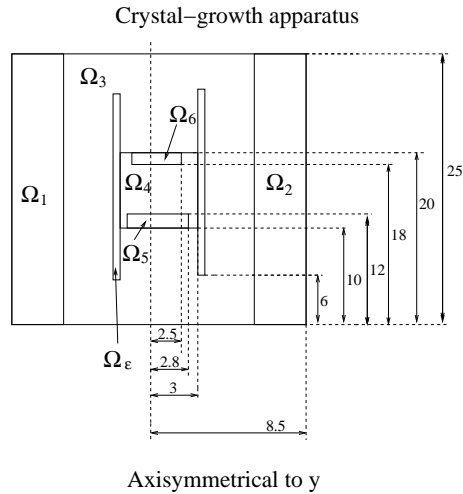


Abbildung 11. 'Geometry 5': The apparatus of the crystal-growth with heat-region ϵ near to the gas-chamber.

MG-Level	Convergence-rate				
	$D_\epsilon = 0.001$	$D_\epsilon = 0.01$	$D_\epsilon = 0.1$	$D_\epsilon = 1.0$	$D_\epsilon = 10.0$
6	0.098	0.075	0.076	0.074	0.078

Tabelle 6. 'Geometry 5': Convergence rates of SCARC on the modified crystal-growth apparatus with $\epsilon = 0.3$ for different diffusion coefficients.

The results of table 6 shows nearly the same convergence-rates for different diffusion operator. Based on the stable local method, also for different geometrical formations the small overlapping methods in combination with the multi-grid method is a strong solver.

5 Conclusions and Discussions

We presented theoretical results for overlapping domain decomposition method which is based on a hierarchy of multigrid methods with highly optimized local smoothing. The error-analysis is based on the Schwarz-waveform relaxation method with a small overlap and an accurate a priori error-estimates. Because of the multigrid concept we could implement a very effective and accurate method. Thanks to the multigrid method the overlap increase for coarser grids and relaxed the errors optimal in each grid-level. Numerical experiments verified our theory and a simple real-life application of a crystal-growth apparatus is presented. In future the combination between multi-level methods and domain-decomposition methods are immense and theoretical results for one-level methods could be used for developing the analysis for the higher level methods.

Literatur

1. Ch. Becker, S. Kilian, S. Turek. *Hardware-oriented numerics and concepts for PDE software*. Future Generation Computer Systems, Elsevier, 22(1-2):217-238, 2006.
2. N. Bubner, O. Klein, P. Philip, J. Sprekels, and K. Wilmanski. *A transient model for the sublimation growth of silicon carbide single crystals*. Journal of Crystal Growth, 205: 294-304, 1999.
3. X.C. Cai. Additive Schwarz algorithms for parabolic convection-diffusion equations. *Numer. Math.*, 60(1):41-61, 1991.
4. X.C. Cai. Multiplicative Schwarz methods for parabolic problems. *SIAM J. Sci Comput.*, 15(3):587-603, 1994.
5. D.S. Daoud, M.J. Gander *Overlapping Schwarz Waveform Relaxation for Convection Reaction Diffusion Problems* Proceeding of DD13 conference, France, published by CIMNE, Barcelona, Spain, April 2002 (first edition).
6. R.E. Ewing. Up-scaling of biological processes and multiphase flow in porous media. *IIMA Volumes in Mathematics and its Applications*, Springer-Verlag, 295 (2002), 195-215.
7. I. Farago, and Agnes Havasi. *On the convergence and local splitting error of different splitting schemes*. Eötvös Lorand University, Budapest, 2004.
8. I. Faragó and J. Geiser. *Operator-Splitting Methods for Multidimensional and Multi-physical Problems in Porous Media*. Comput. Math. Appl., (to be submitted)
9. M.J. Gander and H. Zhao. *Overlapping Schwarz waveform relaxation for parabolic problems in higher dimension*. In A. Handlovičová, Magda Komorníková, and Karol Mikula, editors, *Proceedings of Algoritmy 14*, pages 42-51. Slovak Technical University, September 1997.
10. J. Geiser. *Discretisation Methods with embedded analytical solutions for convection dominated transport in porous media* Proceeding of Numerical Analysis and Applications, Third international conference, Rousse, Bulgaria, 2004, Lect.Notes in Mathematics (Springer), vol.3401, 2005.
11. J. Geiser, R.E. Ewing, J. Liu. *Operator Splitting Methods for Transport Equations with Nonlinear Reactions*. Proceedings of the Third MIT Conference on Computational Fluid and Solid Mechanics, Cambridge, MA, June 14-17, 2005.
12. J. Geiser, O. Klein, and P. Philip. *Anisotropic thermal conductivity in apparatus insulation: Numerical study of effects on the temperature field during sublimation growth of silicon carbide single crystals*. Preprint Weierstra-Institut für Angewandte Analysis und Stochastik, Berlin, 2005.
13. E. Giladi and H. Keller. Space time domain decomposition for parabolic problems. Technical Report 97-4, Center for research on parallel computation CRPC, Caltech, 1997.
14. M.S. Gockenbach. *Partial Differential Equation : Analytical and Numerical Methods*. SIAM, Society for Industrial and Applied Mathematics, Philadelphia, OT 79, 2002.
15. W.H. Hundsdorfer. *Numerical Solution od Advection-Diffusion-Reaction Equations*. Technical Report NM-N9603, CWI, 1996.
16. W. Hundsdorfer and J.G. Verwer. *Numerical Solution of Time-dependent Advection-Diffusion-Reaction Equations*. Springer Series in Computational Mathematics, 33, Springer Verlag, 2003.
17. K.H. Karlsen and N.H. Risebro. *Corrected operator splitting for nonlinear parabolic equations*. SIAM J. Numer. Anal., 37(3):980-1003, 2000.

18. K.H. Karlsen, K.A. Lie, J.R. Natvig, H.F. Nordhaug, and H.K. Dahle. *Operator splitting methods for systems of convection- diffusion equations: nonlinear error mechanisms and correction strategies*. J. Comput. Phys., 173(2):636–663, 2001.
19. S. Kilian, S. Turek. *An example for parallel ScaRC and its application to the incompressible Navier–Stokes equations*. Preprints SFB 359, Nr. 98-06, Universität Heidelberg, 1998.
20. S. Kilian. *ScaRC als verallgemeinerter Mehrgitter- und Gebietszerlegungsansatz für parallele Rechnerplattformen*. Logos Verlag, Berlin, 2002.
21. G.I Marchuk. *Some applicatons of splitting-up methods to the solution of problems in mathematical physics*. Aplikace Matematiky, 1 (1968) 103-132.
22. Gérard A. Meurant. *Numerical experiments with a domain decomposition method for parabolic problems on parallel computers*. In Roland Glowinski, Yuri A. Kuznetsov, Gérard A. Meurant, Jacques Périaux, and Olof Widlund, editors, *Fourth International Symposium on Domain Decomposition Methods for Partial Differential Equations*, Philadelphia, PA, 1991. SIAM.
23. C.V. Pao *Non Linear Parabolic and Elliptic Equation* Plenum Press, New York, 1992.
24. G. Strang. *On the construction and comparision of difference schemes*. SIAM J. Numer. Anal., 5:506–517, 1968.
25. J.G. Verwer and B. Sportisse. *A note on operator splitting in a stiff linear case*. MAS-R9830, ISSN 1386-3703, 1998.
26. Z. Zlatev. *Computer Treatment of Large Air Pollution Models*. Kluwer Academic Publishers, 1995.
27. H.A. Schwarz. *ber einige Abbildungsaufgaben*. Journal fr Reine und Angewandte Mathematik, 70:105–120, 1869.
28. C. N. Dawson, Q. Du, and D. F. Dupont. *A finite Difference Domain Decomposition Algorithm for Numerical Solution of the Heat Equation*. Mathematics of Computation, 57:63-71, 1991